YEARLY TECHNICAL PROGRESS REPORT

submitted to

U. S. Department of Energy

Reporting Periods: 09/2703 – 09/26/04

December 26, 2004

Title: **Intelligent Monitoring System With High Temperature Distributed Fiberoptic Sensor For Power Plant Combustion Processes**

Authors: **Kwang Y. Lee, Stuart S. Yin, Andre Boheman**

The Pennsylvania State University
Department of Electrical Engineering
University Park, PA 16802
Ph. (814) 865-2621, Fax (814) 865-7065
kwanglee@psu.edu

DISCLAIMER

ABSTRACT

The objective of the proposed work is to develop an intelligent distributed fiber optical sensor system for real-time monitoring of high temperature in a boiler furnace in power plants. Of particular interest is the estimation of spatial and temporal distributions of high temperatures within a boiler furnace, which will be essential in assessing and controlling the mechanisms that form and remove pollutants at the source, such as NOx. The basic approach in developing the proposed sensor system is three fold: (1) development of high temperature distributed fiber optical sensor capable of measuring temperatures greater than 2000 C degree with spatial resolution of less than 1 cm; (2) development of distributed parameter system (DPS) models to map the three-dimensional (3D) temperature distribution for the furnace; and (3) development of an intelligent monitoring system for real-time monitoring of the 3D boiler temperature distribution.

Under Task 1, improvement was made on the performance of in-fiber grating fabricated in single crystal sapphire fibers, test was performed on the grating performance of single crystal sapphire fiber with new fabrication methods, and the fabricated grating was applied to high temperature sensor. Under Task 2, models obtained from 3-D modeling of the Demonstration Boiler were used to study relationships between temperature and NOx, as the multi-dimensionality of such systems are most comparable with real-life boiler systems. Studies show that in boiler systems with no swirl, the distributed temperature sensor may provide information sufficient to predict trends of NOx at the boiler exit. Under Task 3, we investigate a mathematical approach to extrapolation of the temperature distribution within a power plant boiler facility, using a combination of a modified neural network architecture and semigroup theory. The 3D temperature data is furnished by the Penn State Energy Institute using FLUENT. Given a set of empirical data with no analytic expression, we first develop an analytic description and then extend that model along a single axis.

TABLE OF CONTENTS

TECHNICAL PROGRESS REPORT

TABLE OF CONTENTS (Continued)

TECHNICAL PROGRESS REPORT

December 26, 2004

Title: **Intelligent Monitoring System With High Temperature Distributed Fiberoptic Sensor For Power Plant Combustion Processes**

Authors: Kwang Y. Lee, Stuart S. Yin, Andre Boheman
Students: J.A. Chavez, S.H. Nam, C. Zhan, Melanie Fox, B.H. Kim, John Valas
The Pennsylvania State University
Department of Electrical Engineering
University Park, PA 16802
Ph. (814) 865-2621, Fax (814) 865-7065
kwanglee@psu.edu
Grant Number: DE-FG26-02NT41532
Performance Period: 09/27/2002 to 09/26/2005

OVERVIEW AND PROGRESS TO DATE

The objective of the proposed work is to develop an intelligent distributed fiber optical sensor system for real-time monitoring of high temperature in a boiler furnace in power plants. Of particular interest is the estimation of spatial and temporal distributions of high temperatures within a boiler furnace, which will be essential in assessing and controlling the mechanisms that form and remove pollutants at the source, such as NOx.

The basic approach in developing the proposed sensor system is three fold: (1) development of high temperature distributed fiber optical sensor capable of measuring temperatures greater than 2000 C degree with spatial resolution of less than 1 cm; (2) development of distributed parameter system (DPS) models to map the three-dimensional (3D) temperature distribution for the furnace; and (3) development of an intelligent monitoring system for real-time monitoring of the 3D boiler temperature distribution.

TASK 1. FIBEROPTIC SENSOR DEVELOPMENT

1.1 Objectives and Motivations

The objective of this task is to develop an innovative high temperature distributed fiber optic sensor by fabricating in-fiber gratings in single crystal sapphire fibers. This unique high temperature distributed fiber optic sensor can precisely monitor the temperature distribution inside a boiler, which, in turn, could substantially increase the burning efficiency and reduce the pollution emission (e.g., NO_x). Figures 1(a) and 1(b) illustrate a power plant and a boiler with embedded fiber optic sensors.

Fig. 1(a) A picture of a power plant
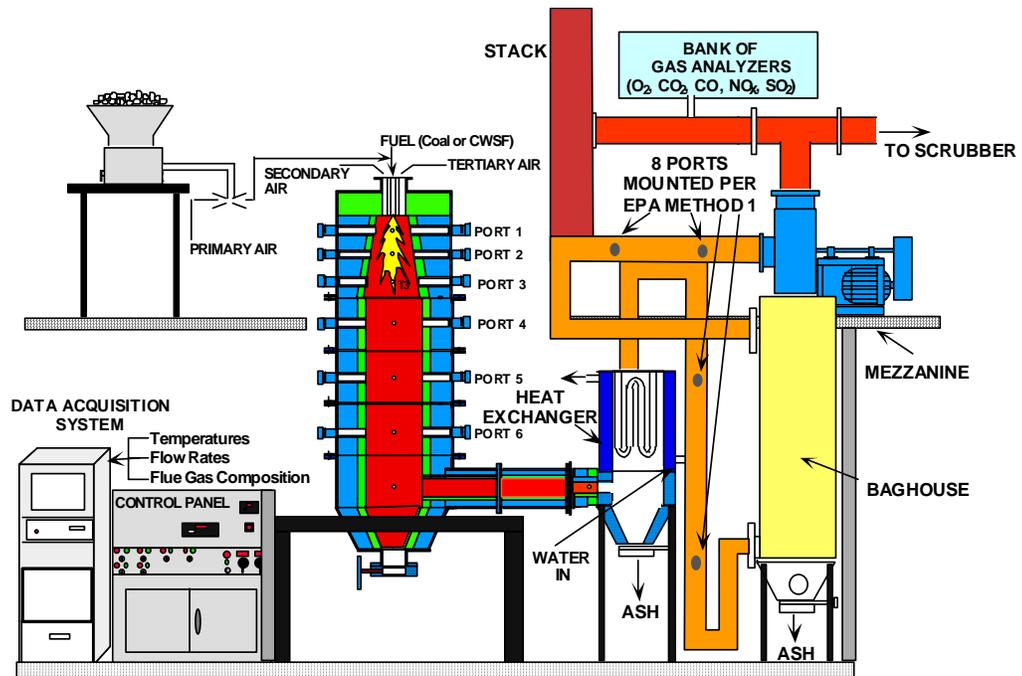
Fig. 1 (b) A boiler with embedded fiber optic sensor.

In the second year, we continuously improve the performance of high temperature distributed fiber optic sensor by using new configuration (such as radiation modal coupling) and new in-fiber grating fabrication approach (such as plasma etching), which can relax the quality requirement (e.g., transparency) on alumina cladding that in turn reduce the complexity for the sensor fabrication and increase practicability of the sensor.

To the best knowledge of authors, so far, no distributed sensors with sapphire fibers have been reported by other groups. For distributed sensors with optical fibers, basically optical time-domain reflectometry (OTDR) or optical frequency domain reflectometry (OFDR)-based methods have been used. With those methods, best achieved spatial resolution was around 1 meter. This means that those standard methods for distributed sensing can not be used for achieving centimeter spatial resolution, which is our case. Another method for distributed sensing is using fiber gratings such as fiber Bragg gratings (FBG) or long period gratings (LPG). Actually, these sensors are multiplexed sensors rather than distributed sensors because they don't provide continuous measurement along the fiber. By multiplexing several sensors, however, a few centimeters spatial resolution can be readily obtained, which has enough resolution in most cases. These 'quasi-distributed'sensors have high sensitivities, simple structures. Unfortunately, this grating-based method can not be directly applied to sapphire fibers due to lack of photosensitivity of sapphire fibers. Micro-machining method might be a logical solution for gratings in sapphire fibers because the only way to perturb refractive index of the fiber without photosensitivity is to mechanically change the shape of the fiber.

1.2 Major Accomplishments

1.2.1 Demonstrate the effect of micro-machined gratings on single crystal sapphire fibers.
We showed that the micro-structuring is possible either by mechanical dicing or chemical etching after the patterning by lithography in the last year report. To demonstrate the effect of micro-machined gratings, we conducted following experiments.

- To fabricate in-fiber grating with large depth, we used mechanical dicing approach. In the experiment, a 5 cm long single crystal sapphire fiber, with 250 micron diameter, was used. In order to hold the fiber, the fiber sample was attached to a 2" x 2" glass substrate with the use of Crystalbond 509 adhesive and a hot plate. The glass substrate was then placed on a computer-controlled chuck underneath a diamond saw blade. The substrate was firmly held by the vacuum chuck once it was properly aligned. The blade width was 40 micron and the grating pitch was 100 micron. The number of the notches was one hundred. The depth of the grating was 30 micron. After finishing the dicing, the glass substrate was heated on the hot plate and the sapphire fiber samples were carefully taken out of the substrate and cleaned with acetone.

- Figure 2 shows the fabricated grating using dicing approach. As we can see from the figure, overall structures were well formed but the edges of the notches were not smooth. This is the limitation of dicing approach. But it provides simple and fast means for micro-machining.
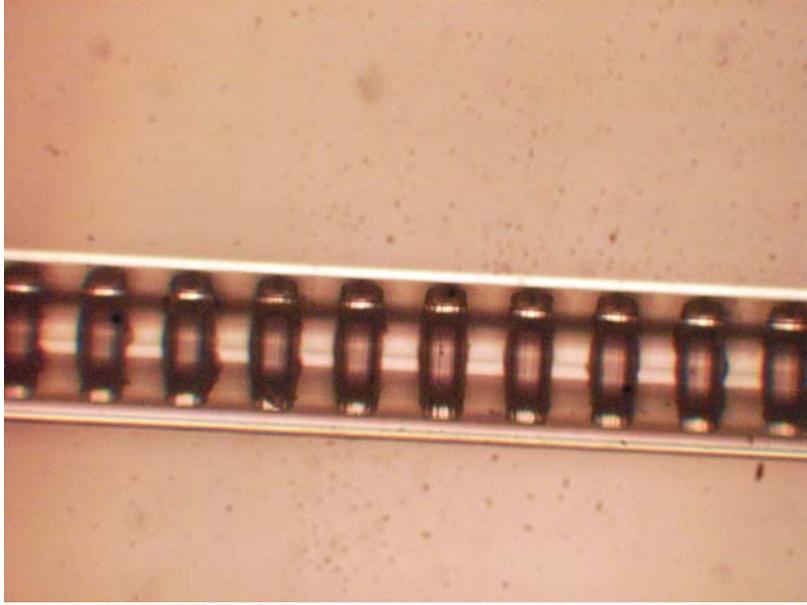
Fig. 2 Fabricate in-fiber long period grating in single crystal sapphire fiber by precise dicing.

- To see the effect of the micro-machined fiber, we built the experimental setup as shown in Fig. 3. The light source was HP 8168E tunable laser. As the output of the tunable laser was connectorized with FC/PC, collimating optics was used to collimate the beam coming out of the connector end. NEW FOCUS model 9091 five-axis fiber aligner was used for this purpose. The collimated light beam was focused on the one end of the sapphire fiber sample by a microscope object lens (x20). The output beam of the sapphire fiber was directly coupled to a regular multimode fiber which was connected to HP 70951B optical spectrum analyzer (OSA). To get the optimum beam coupling between the fibers, Newport 462 series precise 3 axis aligner was used. A sample chamber was made to contain the index matching oil for the cladding of the sapphire fiber. The fiber sample penetrated this chamber and the index matching oil was provided through top open cover.

.

- For the micro-machined gratings to work as long period gratings (LPG), well defined uniform cladding layer has to be formed. Circumventing this problem, one of the ways for watching the effect of micro-machined gratings is to observe radiation coupling assisted by the gratings. A simple slab waveguide model can be used to explain this effect. If the periodic perturbation is to couple the light from the guided mode to a wave propagating into the surrounding cladding and making angle θ with the direction of propagation as shown in Fig 4(a), then we must have the following relation as shown in Fig. 4(b).

$$\beta - K = k_0 n_s \cos\theta$$

where $\beta = 2\pi n_{eff} / \lambda$ (propagation constant), $K = 2\pi / \Lambda$ (grating vector).

When this, so called, quasi-phase matching condition is satisfied, the radiation coupling from the guide mode to cladding occurs. Fig 4(c) shows the calculated wavelength dependence of radiation angle according to the quasi-phase matching condition. In the calculation, the effective refractive index of core is assumed to 1.78. The region below 0˚ angle means that no radiation coupling is allowed. As we can see from the graph, when the refractive index of the cladding is 1.765, the radiation coupling occurs for the longer wavelength than 1550 nm. This model gives us good qualitative explanation for the case of sapphire fiber. For a certain refractive index of cladding, the radiation coupling will occur for longer wavelength than a specific value.
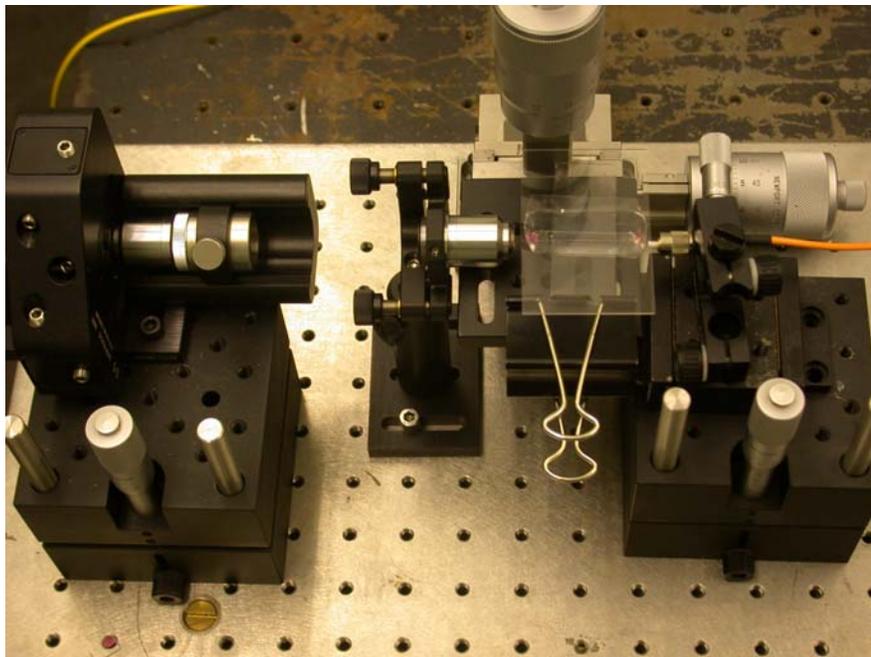
Fig 3. The experimental setup for measuring radiation-mode coupling effect by micro-structured gratings in the sapphire fiber

- While changing the refractive index matching oil (Cargille Laboratories, refractive index liquids M series) for the cladding of the fiber in the chamber, output spectrums were observed. The measured spectrums are shown in Fig. 4. With air cladding and 1.79 index cladding, the spectrums didn't change much. When the refractive index was 1.795, we can see the grating-assisted radiation coupling took place in the longer wavelength region (>1540nm). With 1.80 index cladding, output light has almost disappeared. Note that the values of refractive index of the index matching oil are dependent on the wavelength. The provided values by the manufacturer were measured at visible wavelength. The measured

coupling efficiency of the grating was very low, which is believed due to the inaccuracy of dicing saw (normally nanometer order accuracy is required) and surface roughness.

(a)   (b)
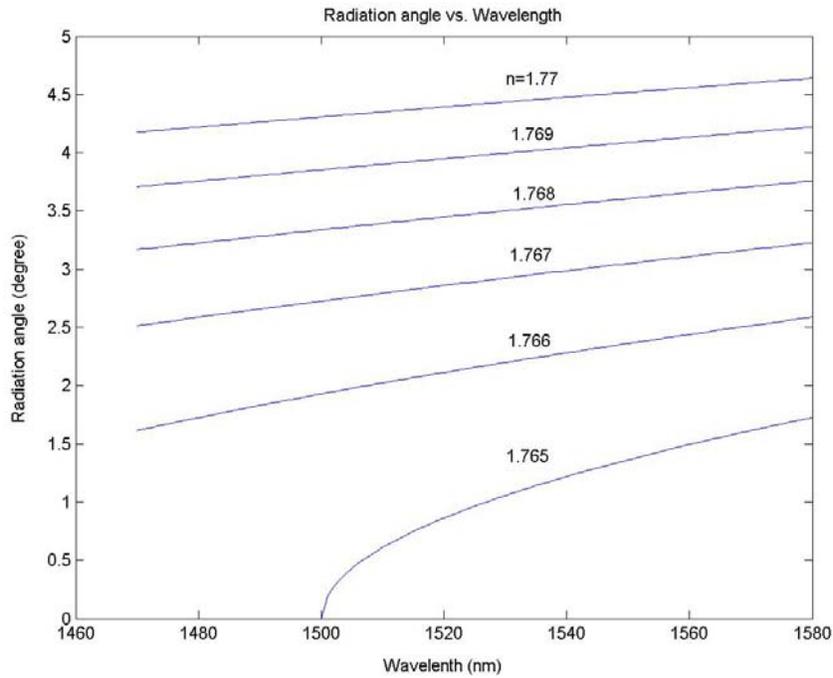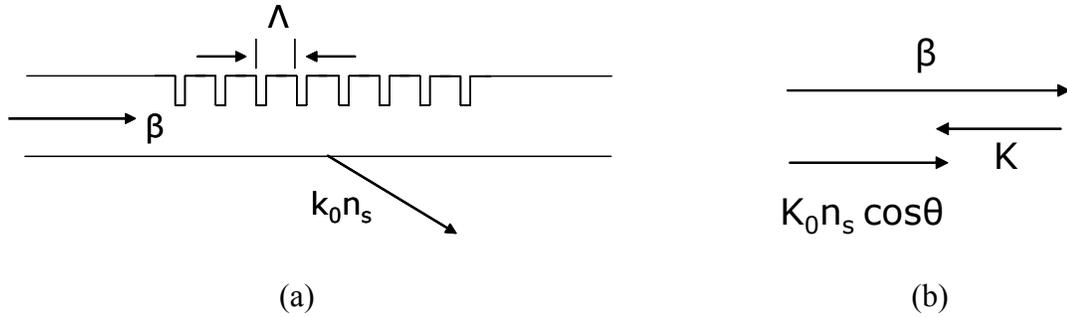
(c)

Fig. 4 Wavelength dependence of radiation mode coupling

1.2.2 Demonstrate the possibility of using super continuum highly broad band source

In general, the number of grating-based multiplexed fiber sensors is limited by the bandwidth of the source. The bandwidth of normal tunable source is around 100 nm. To increase the number

of multiplexed sensors, we need wider bandwidth for the light source. A supercontinuum light could be a solution for large scale sensor systems. Supercontinuum generation can be achieved in a photonic crystal fiber. Since the core radius of a certain photonic crystal fiber can be only 1~2 micron order, nonlinear effects to cause the supercontinuum are greatly enhanced and the white light generation process easily takes place with much less input light intensity. Figure 6 shows the experimental setup for supercontinuum generation and generated white light source. The measured spectrum was across the entire bandwidth of OSA (600~1700nm). As the spectral fluctuation of the generated white light frequently occurred by small disturbance of input coupling, it couldn't be used as an actual light source for the sensor. Once this problem is resolved, it will be a promising candidate for large scale sensor array system.
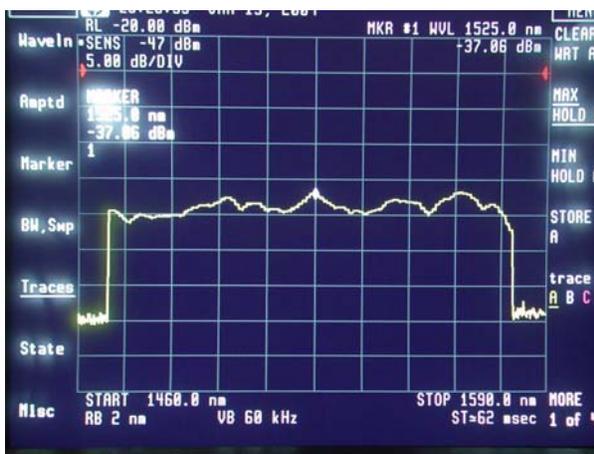
(a) air
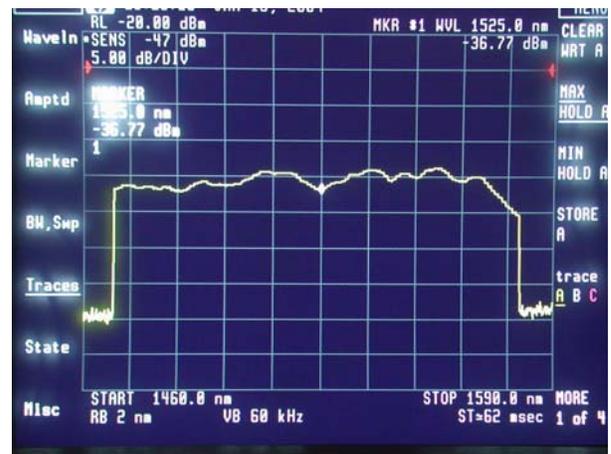
(b) 1.79

(c) 1.795

(d) 1.80

Fig. 5 The output spectrum of the sapphire fiber with surface gratings
for different cladding refractive indices.
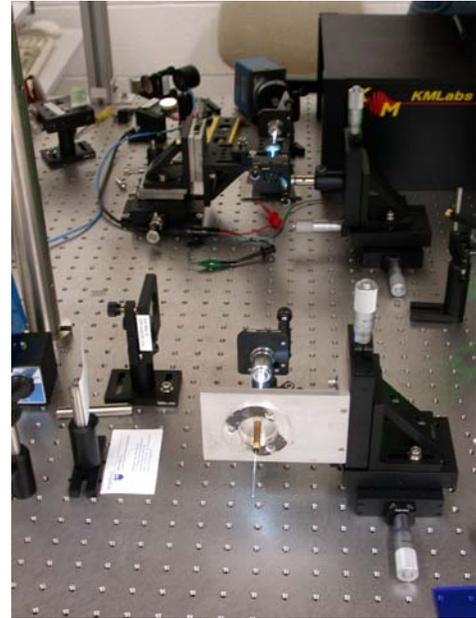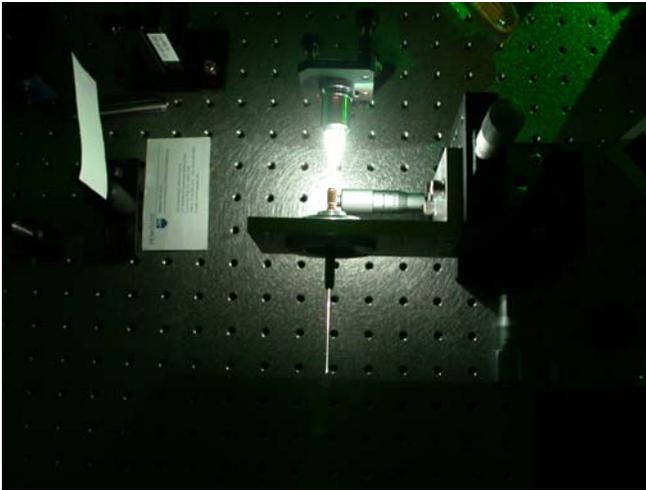
Fig. 6 Supercontinuum white light source generation for fiber sensor systems.

<u>1.2.3 Investigate the more accurate patterning and micro-structuring method than mechanical dicing.</u>

So far, the problems we've encountered are

- Poor spatial resolution of mechanical dicing method
- Shallow grating depth of chemical etching method
- Surface roughness of structured fiber

Especially, if want to make fiber Bragg grating (FBG) in the sapphire fibers, we need sub-micron patterning (~ 200nm) capability. To resolve those problems, we investigated a new fabrication method using the following fabrication steps, which is illustrated in Fig. 7.

- Fine polishing
- Lithography or e-beam lithography
- Mask patterning

- High density plasma etching (ICP-RIE)
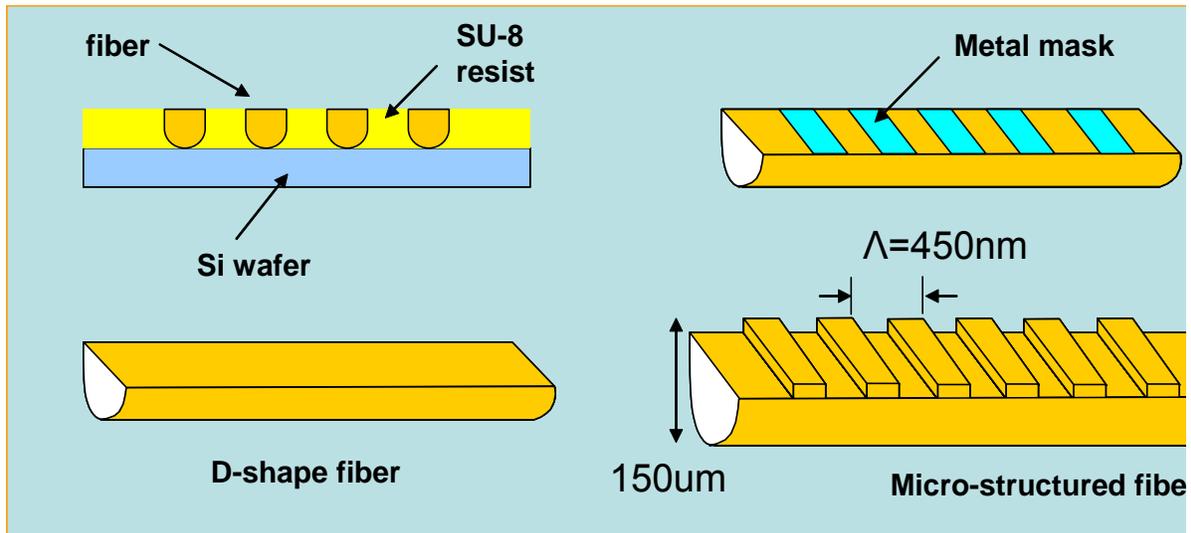
Figure 7 An illustration of a fabrication process for sapphire fiber FBG grating
by plasma etching.

For the accurate patterning, the precise lithography process is required, which means well polished flat surface is needed for spin coating uniform photoresist layer over the sample. It can be accomplished by putting the fibers on the silicon wafer, filling the gap with thick negative photoresist SU-8, post-baking the resist and then polishing the surface. The fibers will have D-shape as the result of polishing step. Once the surface is made flat, we can use the standard micro-fabrication methods. Using normal lithography or e-beam lithography method, the accurate pattern can be defined in the photoresist layer. For transferring the pattern into the sapphire fiber, high density plasma etching (ICP-RIE) process can be used. With $BCl_3:Cl_2$ chemistry and 800 W RF power, the etch rate of sapphire can reach 350nm/min.

1.3 Future Work Plan

We will apply the developed high temperature distributed fiber optic sensor systems in the furnace testing.

TASK 2: BOILER FURNACE MONITORING MODEL DEVELOPMENT

2.1 Objectives and Motivations

Development of the multi-dimensional combustion simulation model has been the focus of activities by Prof. Boehman and his student. The effort has primarily been to get a functional workstation, with CFD software, into place and to train the student on its application to multi-dimensional combustion simulation.

The graduate student is now working with a 2-D model of the Down Fired Combustor Modeling this boiler has provided the graduate student the opportunity to become skilled using FLUENT, to leverage existing grids and extensive prior experimental work for comparison. This represents a shift from the initial direction, which was to work on a 3-D simulation of the Demonstration Boiler. Subsequent applications of FLUENT will extend to the Drop Tube Reactor (DTR) and the Demonstration Boiler.

The student has become proficient at using Gambit 2.1.6, the grid generation software for FLUENT, in preparing the demonstration boiler grid for simulation. Specific skills include:
- o discretizing grid volumes
- o meshing complex geometries
- o evaluating grid for skewness
- o grid refinement
- o creating mesh for data collection at desired spatial positions

The student has also acquired skills in FLUENT, specifically:
- o prePDF generation (for combustion simulations)
- o solver selection
- o premixed & non-premixed systems
- o steady state or transient simulations
- o air-staging
- o knowledge to carry out validation studies

2.2 Major Accomplishments

The hypothesis of this work is that a series of one dimensional, line-of-site temperature profiles will provide in-situ temperature information sufficient to predicting NOx emissions at the boiler exit, based on the degree of stratification within the combustor, and the relationship between stratification to NOx formation.

The desire to implement a temperature measurement-based monitoring and feedback control system for improved NOx control necessitates the discovery of a functional correlation between boiler temperature distributions, boiler operating parameters and NOx formation. This numerical modeling effort serves to determine how best to implement temperature profile information that can be obtained in real-time with a novel fiber optic sensor, which can provide a measurement of the temperature distribution along a line-of-site through the interior of the boiler. This work will be successful if information from 1D lines-of-site can be used to develop a numerical

relationship between temperature and boiler exit NOx emissions, and that implementation of that relationship provides unique exit NOx concentrations from the measured temperatures, for the group of temperature profiles from each case tested.

2.2.1 The Demonstration Boiler

The Demonstration Boiler, an industrial boiler located at Penn State's Energy Institute, originally designed for fuel oil or natural gas feedstock, but has since been modified to run coal-based fuels, was modeled in this study; it is. The D-type watertube boiler has a capacity of 15,000 lb/h steam at 300 psig, with approximate dimensions of 2.6 x 1 .8 x 2.6 meters. The burner configuration is shown in Fig. 1.
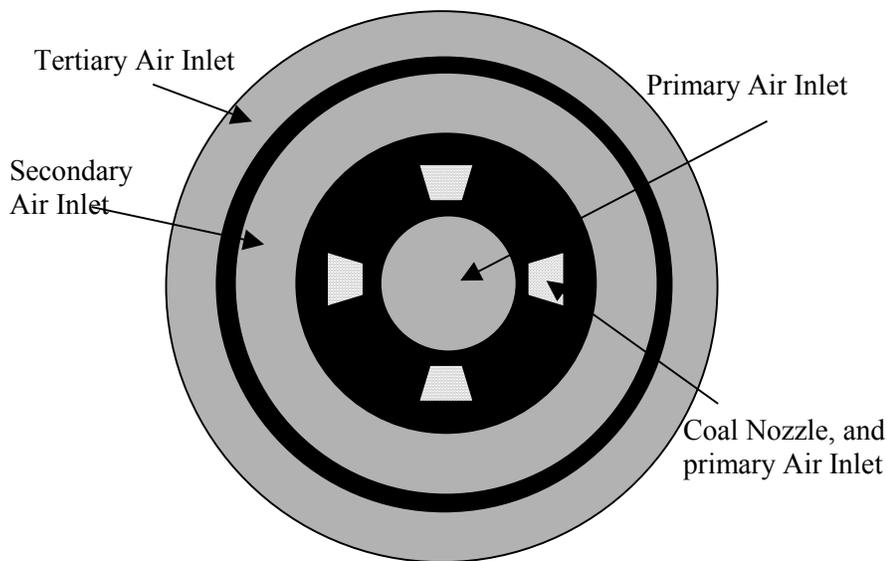
Fig. 1. Burner Configuration

2.2.2 Test Matrix

Two different sets of tests were performed. The first set of tests comprised two combustion simulations, for which operating parameters are specified in Table 1. A series of four tests were completed in the second study. The differences between the two studies are summarized in the model specifications section, and swirl was applied to the tertiary flow in the second set of tests, shown in Table 2.   The rationale for modifying the operating conditions (and the model selections) for the Group B simulations, compared to those of Group A, was to improve the conditions in order to model combustion more accurately, and to match operation conditions from real experiments in order to validate the combustion results.

Table 1. Test Matrix: Group A – Boiler Inlet Conditions

	Case 1	Case 2
Fuel Type	General	General
Fuel Rate (kg/s)	0.17	0.17
Primary Air Rate (kg/s)	0.20	0.20
Secondary Air Rate (kg/s)	0.53	0.20
Tertiary Air Rate (kg/s)	1.23	1.56
Total Air Rate (kg/s)	1.96	1.96
Fuel Temperature (K)	300	300
Air Temperature (K)	464	464
Swirl Number	None	None

Table 2. Test Matrix: Group B – Boiler Inlet Conditions

	Case 1	Case 2	Case 3	Case 4
Fuel Type	Kentucky	Kentucky	Kentucky	Kentucky
Fuel Rate (kg/s)	0.17	0.17	0.17	0.17
Primary Air Rate (kg/s)	0.20	0.20	0.20	0.20
Secondary Air Rate (kg/s)	0.550	0.200	0.375	0.725
Tertiary Air Rate (kg/s)	1.240	1.590	1.415	1.065
Total Air Rate (kg/s)	1.99	1.99	1.99	1.99
Fuel Temperature (K)	400	400	400	400
Air Temperature (K)	1800	1800	1800	1800
Swirl Number (Tertiary)	0.4	0.4	0.4	0.4

2.2.3 Grid Development

The computational grid comprises multiple, distinct cells, that represent the continuous flow field. Each cell or volume is treated separately, though the sum of cells represents the whole. The grid governs the accuracy and the stability of the calculation, and therefore must be designed carefully.

A three-dimensional, non-uniform grid was generated to represent the burner and furnace (entire boiler). The complexity of the burner geometry imposed restrictions as to how the furnace area could be constructed. A visual representation of the grid, comprising more than 270,000 nodes, is shown in Fig. 2.
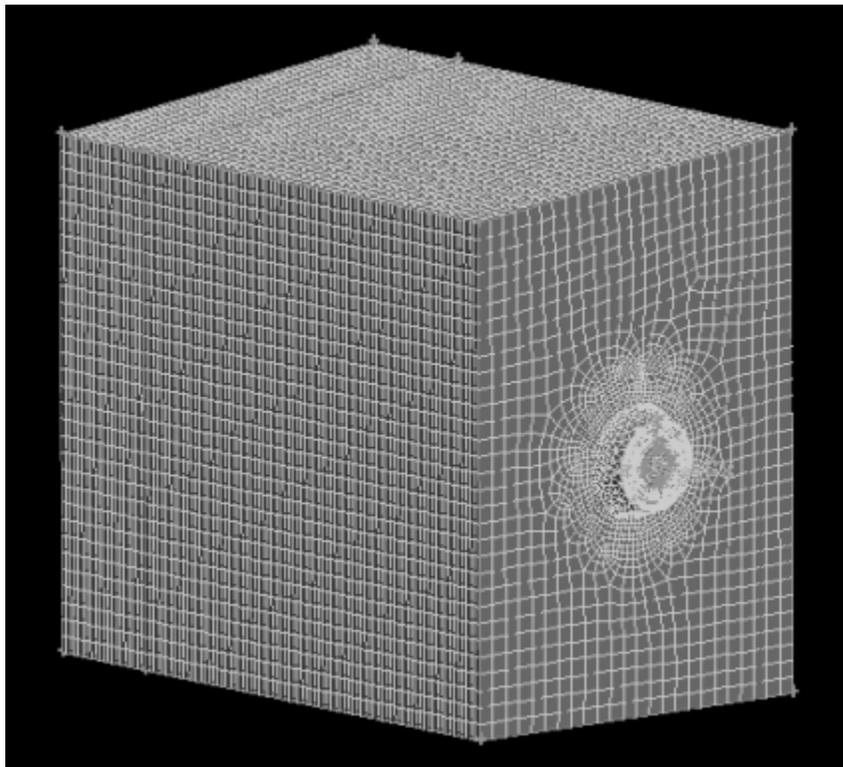
Fig. 2. Computational Grid

2.2.4 Results: Group A

Temperature profiles of 2D planes throughout the boiler were examined from the final
calculations, examples of such profiles are shown in Fig. 3 and Fig. 4. The evidence of
stratification of combustion within the boiler determined the proposed sensor locations, shown in
Fig. 5. Temperature and NOx data along 1D lines of site were extraction from the combustion
calculations, for example, as shown in Fig. 6.

Fig. 3. Temperature Profile (horizontal) – Case 1

2.09e+03	
2.00e+03	
1.92e+03	
1.84e+03	
1.76e+03	
1.68e+03	
1.59e+03	
1.51e+03	
1.43e+03	
1.35e+03	
1.27e+03	
1.18e+03	
1.10e+03	
1.02e+03	
9.37e+02	
8.55e+02	
7.73e+02	
6.91e+02	
6.09e+02	
5.27e+02	
4.45e+02	
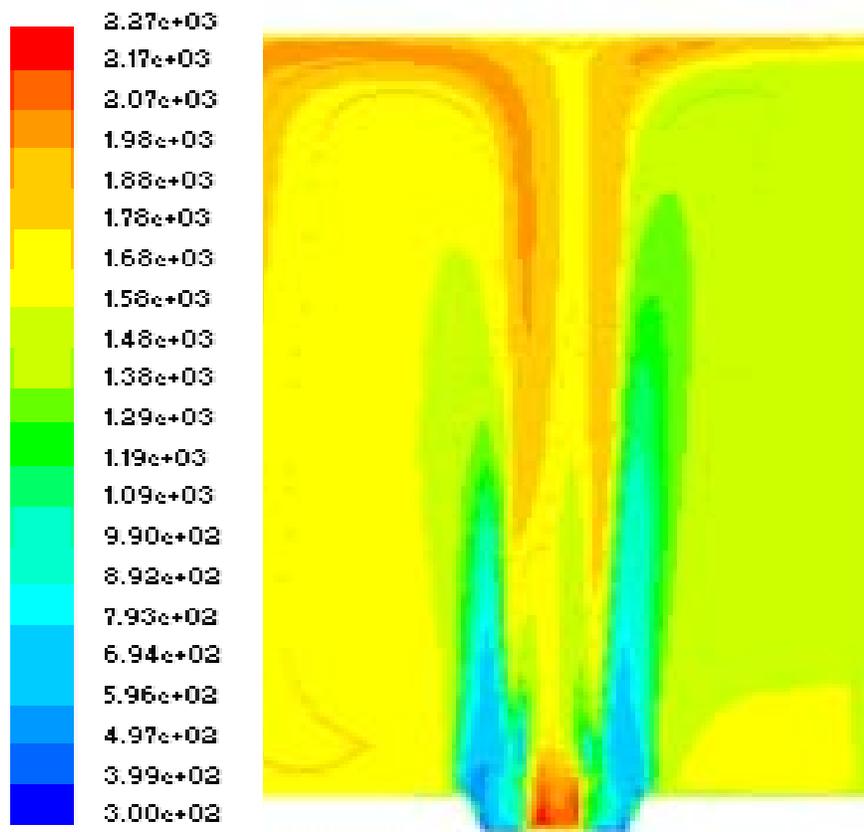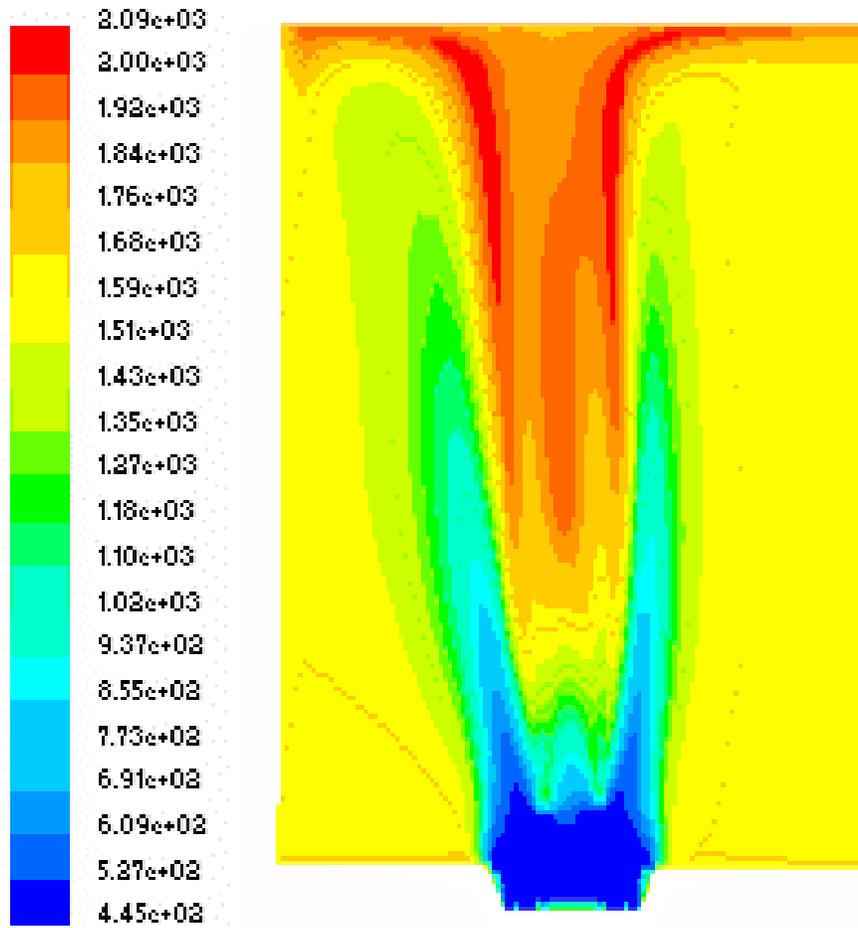
Fig. 4. Temperature Profile (horizontal) – Case 2
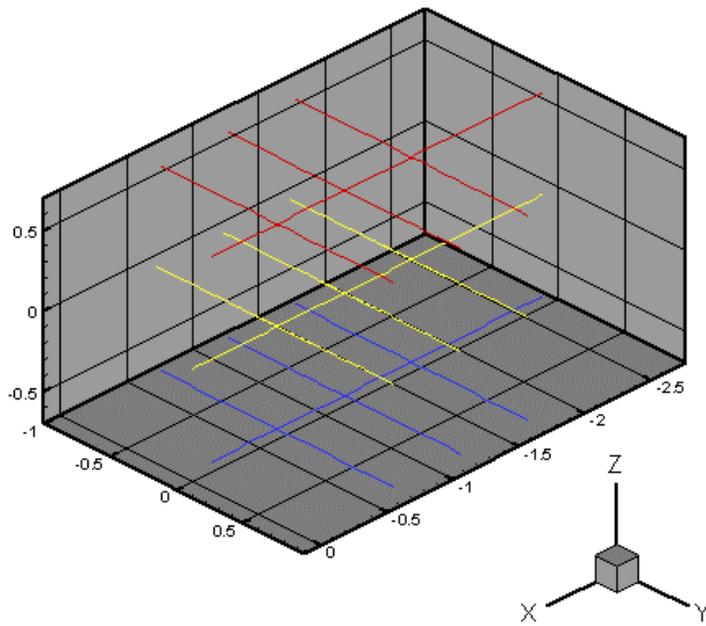
Fig. 5. Spatial Description of 1D Sensors – Test A
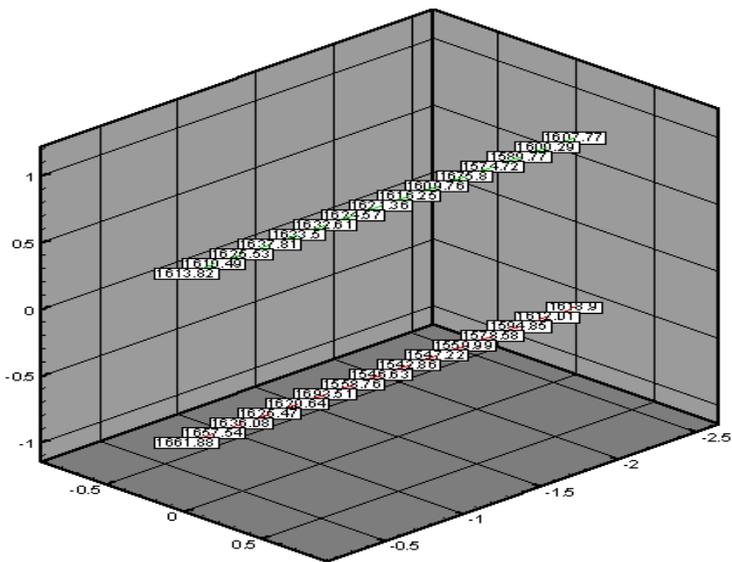
Fig. 6. Temperature (K) –Case 2

2.2.5 Conclusions

The findings of this investigation conclude that in-situ temperature measurements within a combustor are not sufficient to predict NOx emissions at the boiler exit. This technique may be implemented within a regular burner, capable of air staging, but without swirl. In that case, oxidative chemistry is the primary route for NOx formation, and it can be related linearly to temperature. However, this technique showed promise in a very simple combustion system that cannot be assumed to be "accurate" at this time. "Real-life" combustion systems will include eddies and vortices that the grid may not have enabled, or that were not modeled due to simplicity of the model specifications.

The technique is not useful for air-staged combustion systems with swirl, according to the analysis performed in this study. Swirl creates fuel rich recirculation zones, where temperatures can be high enough to suggest increased NOx formation, but instead decrease NOx formation as a result of insufficient stoichiometry.

2.2.6 Recommendations

In order to better comprehend the results of this work, and to examine possibilities not investigated herein, it is proposed the following studies be conducted:
- Validation study and stability analyses of the models employed.
- Mesh refinement studies of the existing grid, in order to assure the computational region appropriately represented the boiler, and to guarantee that the mesh spacing was adequate to detecting swirl and its effects. Coarsening areas of the grid where appropriate may save computational time.
- Improved combustion calculations, including a 2-stream PDF model, prompt NOx formation, and more accurate swirl representation.
- A comprehensive study of the behavior within the boiler, in order to determine the most appropriate spatial location for the 1D sensors.
- Determination of ability of a complex algorithm to link in-situ temperature information to exit NOx concentrations. The algorithm could survey the sensor reading for the most stratification, and eliminate the temperature information outside the bounds of the stratified areas, and then use the selected information to look at possible correlations between temperatures and exit NOx.
- Investigation of an algorithm based on the frequency of certain temperature values, or the frequency of series of temperature for a given sensor, may also be useful.

2.3 Future Work Plan

The Demonstration Boiler, an industrial boiler located at Penn State's Energy Institute will be modeled using FLUENT and the 1D temperature measurement will be compared with the simulation. The 3D temperature distribution will be compared with the result of extrapolation by the system-type neural networks to be developed in Task 3 as an intelligent monitoring system for estimating temperature distribution in boiler furnace.

TASK 3. INTELLIGENT MONITORING SYSTEM DEVELOPMENT

3.1 Objectives and Motivations

The proposed project will focus on an investigation of a mathematical approach to extrapolation, using a combination of system-type neural network architecture and the semigroup theory. The target of the investigation will be a class of distributed parameter systems for which, because of their complexity, lack an analytic description. Although the primary objective is extrapolation, this effort must begin with the development of an analytic description from the given empirical data, and then, proceed to extend that model into an adjoining domain space for which there is neither data nor a model. That is, given a set of empirical data for which there is no analytic description, we first develop an analytic model and then extend that model along a single axis. Semigroup theory provides the basis for the neural network architecture, the neural network operation and also for the extrapolation process. Concerning the architecture, semigroup theory dictates that under certain circumstances, a given composite mapping should be regarded as two families of maps, requiring two separate neural network channels; concerning the operation, semigroup theory requires that the second channel possesses the classic semigroup property of mapping composition; concerning the extrapolation process, semigroup theory requires that the extrapolated elements share the same semigroup property that are possessed by the elements previously formed from the given empirical data. The semigroup theory provides a unified and a powerful tool for the study of differential equations on Banach space, covering system described by ordinary differential equations, partial differential equations, functional differential equations and combinations thereof [1]. For applications to control systems, estimation techniques are often required to compensate for an inadequate amount of data, arising from the unavailability of that data.

In the past, for systems described by ordinary differential equations, various estimation techniques have been developed with the most popular (and successful) ones being based on variations of the Kalman filtering theory. However, as control theory has been expanded to include more complex behavior, such as distributed parameter systems, described by partial differential equations, the estimation problem has taken on a new importance, because now it is necessary to provide estimated data at a great (theoretically infinite) number of points. A need therefore exists for a generalized estimation technique that can be applied to a broad class of nonlinear systems, any one of whose behavior is described by a partial differential equation. Stated very concisely, a need exists for a technique which can begin with a sparse set of data derived from a few discrete points within some continuum in one, two or three dimensional space and which can then develop estimated data at as many points as needed within the continuum, in a manner which is dynamically consistent with the given empirical data points, and additionally, to extrapolate the resulting function into an adjoining region of space for which there is no data.

The modeling technique uses a process referred to as algebraic decomposition to find a particular type of smooth approximating function to the empirical data, namely, one that lends itself to a representation as the product of a coefficient vector and a basis set of functions, where the coefficient vector possesses a semigroup property. Extrapolation involves only the coefficient vector and begins by training the semigroup channel neural network to replicate the coefficient

vector trajectory, while at the same time acquiring a semigroup property of its own (expressed in weight space). The acquisition of the semigroup property is dynamic, expressing itself as a particular sequence of weight changes. The learning algorithm is new in that the weight convergence is realized recursively, by training the neural network repetitively over successively longer intervals and searching for a second level of convergence. Extrapolation is concerned with discovering the dynamics of the weight change sequence and then autonomously continuing that sequence.

3.2 Development of Intelligent Monitoring System

3.2.1 Monitoring of Temperature Distribution in Boiler Furnace

The electric utility industry is charged to deliver power as inexpensively and as reliably as possible. Meeting these dual obligations has become increasingly difficult over the past 30 years. Environmental and economic concerns pressed the utility industry to develop clean and efficient ways of burning coal and oil. This has required major improvements in instrument, data management, and control of electric power plant components such as boilers. It has become a challenge to measure high temperature distributions of high-pressure liquids, steam, combustion gases, and heat transfer components in extremely adverse power plant environments. Traditional sensors have not exhibited sufficient stability and long-term accuracy without requiring expensive maintenance and recalibration. Intelligent distributed parameter estimation coupled with the fiberoptic sensor system is to be developed to better estimate the temperature distribution of a boiler furnace and for improved combustion. The basic approach in developing the proposed monitoring system is two fold: (1) development of distributed parameter system (DPS) models to map the three-dimensional (3D) temperature distribution for the furnace; and (2) development of an intelligent monitoring system for real-time monitoring of the 3D boiler temperature distribution based on the 1D fiberoptic sensors.

Fig. 1(b) in Task 1 shows the Penn State down-fired combustor (DFC), which is an advanced pilot-scale furnace designed to evaluate the combustion performance of various fuels (natural gas, coal, coal-water slurry fuel) including emissions monitoring. The combustor has a 20-inch internal diameter, is 10 feet high, and is designed for a thermal input of 350,000 Btu/h (nominal), but this can be varied from 200,000 to 500,000 Btu/h. The nominal temperature range is from 1,200 to 1,600 °C.

The proposed boiler furnace-monitoring model addresses the estimation of spatial temperature distribution continuously for any operating condition. The three-dimensional (3D) distributed parameter systems (DPS) model, however, is highly nonlinear and time varying with significant uncertainties in model parameters. Therefore, an efficient state estimation methodology will be developed for this class of DPS models. A three-dimensional DPS model is described by a set of partial differential equations (PDE's) for temperature distribution in 3D spatial domain. State estimation technique has matured for lumped parameter systems, that is, the systems described by ordinary differential equations (ODE's), primarily due to the Kalman filtering theory. Parallel attempts have been made for DPS [2]; however, its application has been limited due to the complexity of the model. As an alternative to the above model-based estimation techniques, such as infinite dimensional extended Kalman filtering, an intelligent monitoring scheme will be

developed for 3D temperature estimation by using the proposed system-type neural networks. Commercial grade simulation codes such as FLUENT will also generate 3D temperature data to train the neural networks. Then, an intelligent algorithm will be developed to adaptively tune the monitoring system in real-time to implement in the experimental boilers. Much work on computational intelligence has already been performed at the Penn State Intelligent Distributed Controls Research Laboratory (IDCRL) [2]. The previous emphasis on the application of computational intelligence for control and diagnostic will be shifted to state estimation and prediction problems.

3.2.2. Failures/shortcomings of Conventional ANN's

Recently, a shift has occurred in the overall architecture of neural networks from simple or component-type networks to system-type architectures. The most popular architecture seems to be the one advocated by Jacobs and Jordan [4], called the "Modular Connectionist Architecture", one example of which is shown in Fig. 1 [5]. It consists of a collection of expert components, each being trained independently, tied together by a component called the "gating logic" element, whose function is to decide on the relative contributions to be made by each expert component, such that when they are added, they provide the correct output for a given input. The present proposed method represents an adaptation of Fig. 1.

The most serious flaw in the design of system-type neural networks is the lack of a cohesive discipline in the architectural design and in the design of the learning algorithm. Virtually, the entire design is done on an intuitive basis. As a contrast to intuition, the proposed method relies on semigroup theory for the design of the semigroup channel.


$$Z = \sum_{i=1}^{N} G(i)Y(i)$$
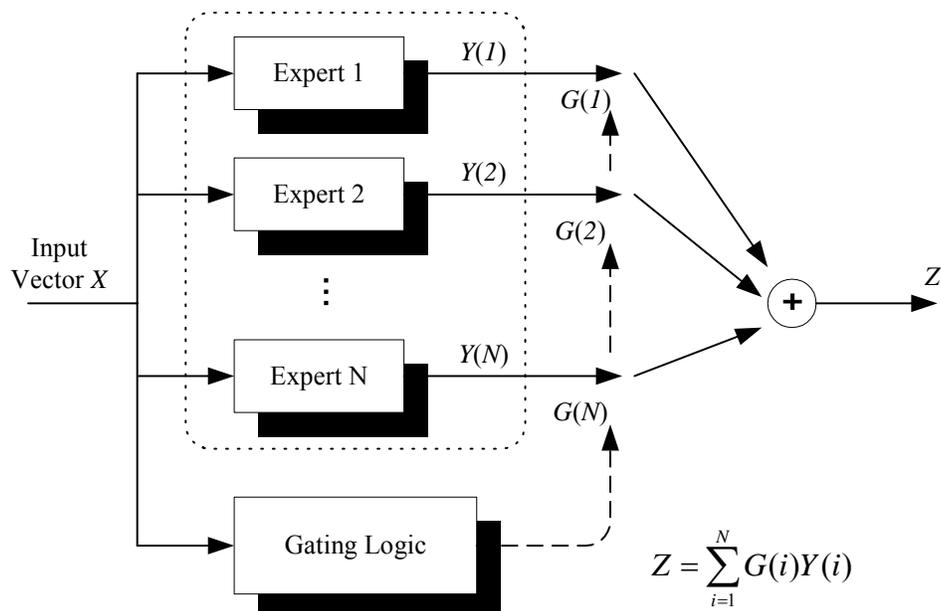
Fig. 1 Modular connectionist architecture.

To illustrate the lack of a cohesive discipline, in [5], the partitioning of components corresponds to separation of variables, which works if the variables are separated and does not work if the variables are not separated. C. Relationship of semigroup theory to ANN design

3.2.3 Semigroup Theory

In recent years, among many other applications, semigroup theory has been widely used in the study of control and stability of systems governed by differential equations on an abstract Banach space. It is well known that differential equations form a major tool in the study of pure and applied sciences including engineering and many areas of social sciences. Depending on the problem, these equations may take various forms, such as functional differential equations, partial differential equations (PDE's), and sometimes combination of interacting systems of ordinary and partial differential equations. In general, under broad assumptions, many of these equations can be reformulated as ordinary differential equations on abstract spaces, for example, Banach spaces. Once this is done, various "denseness" theorems then provide the basis for forming a finite-dimensional approximation. This is where semigroup theory plays an important role and provides a unified and powerful tool for the study of existence, uniqueness, and continuous dependence of solutions on parameters and their regularity properties. Semigroup theory has also found extensive applications in the study of Markov process, ergodic theory, approximation theory and control and stability theory [1]. To give an idea of a semigroup property being possessed by a mapping, consider the following steady state heat flow model in Cartesian coordinates:

$$\frac{\partial^2 T}{\partial x^2} + \frac{\partial^2 T}{\partial y^2} = 0 .$$

If we set $T(x,y) = C(y)^T E(x) = c_1(y)e_1(x) + c_2(y)e_2(x)$, where e_i are orthonormal basis, then by substitution, $c_1'' e_1 + c_2'' e_2 = -c_1 e_1'' - c_2 e_2''$. This, in turn implies

$$c_1'' + c_2'' <e_2,e_1> = -c_1 <e_1'',e_1> -c_2 <e_2'',e_1> \\ c_1'' <e_1,e_2> +c_2'' = -c_1 <e_1'',e_2> -c_2 <e_2'',e_2> , \quad \text{or} \quad \begin{bmatrix} c_1'' \\ c_2'' \end{bmatrix} = A \begin{bmatrix} c_1 \\ c_2 \end{bmatrix}$$

for a suitable matrix A, which leads to a semigroup for $C(y)$.

3.2.4 Relationship of Semigroup Theory to Neural Network Design

The semigroup approach [6] begins by asserting that certain functions are to be re-interpreted as follows: under certain circumstances, the function $T(r,z)$ should be thought of not as one map, but rather, as one family of maps: $\{T_z(r), z \in [0,L]\}$ which, in turn, is produced by a second family of maps $\{\Phi(z)\}$ where the two families are related by the following:

$$T_z(r) = C(z)^T E(r); \quad \text{where:} \ C(z) = \Phi(z)C(0), \text{ and where:} \Phi(z_1 + z_2) = \Phi(z_1)\Phi(z_2) .$$

This interpretation suggests that the mapping must be achieved with a pair of neural networks, one that selects a given function at each value of z and another that then implements the chosen

function. This interpretation also places severe constraints on the "selecting" neural component, forcing it to take on the generic semigroup behavior: $\Phi(z_1 + z_2) = \Phi(z_1)\Phi(z_2)$.

If a given system behavior (expressed as a set of data) possesses a semigroup property, the extrapolation of that data set is achieved by a neural network (the semigroup channel) which itself acquires its own semigroup property. The semigroup property is ultimately achieved within the semigroup channel as a sequence of weight changes that occur after weight convergence has taken place.

3.2.5 Proposed Neural Network Architecture.

Neural networks are being used for systems described by PDE's [7]. The system-type attribute of the neural network architecture is shown in Fig. 3, implementing an arbitrary function $T(z,r)$. Unlike conventional neural network architectures that would attempt to achieve the mapping $T(z,r)$ with one neural network, the proposed architecture reflects a system-type approach using two neural network channels, a Function Channel and a Semigroup Channel, in an adaptation of the connectionist architecture (Fig. 2). During use, the semigroup channel supplies the function channel with a coefficient vector $C(z)$ as a function of the index z. The coefficient vector, when applied to the basis set $E(r)$ of the function channel, causes the function channel to operate as one specific function from within a vector space of functions. Jointly, these two channels realize a semigroup-based implementation of the mapping $T(z,r)$. The similarity between the proposed architecture (Fig. 2) and that of Fig. 1 arises from the fact that the Function channel is implemented as N "expert" systems.
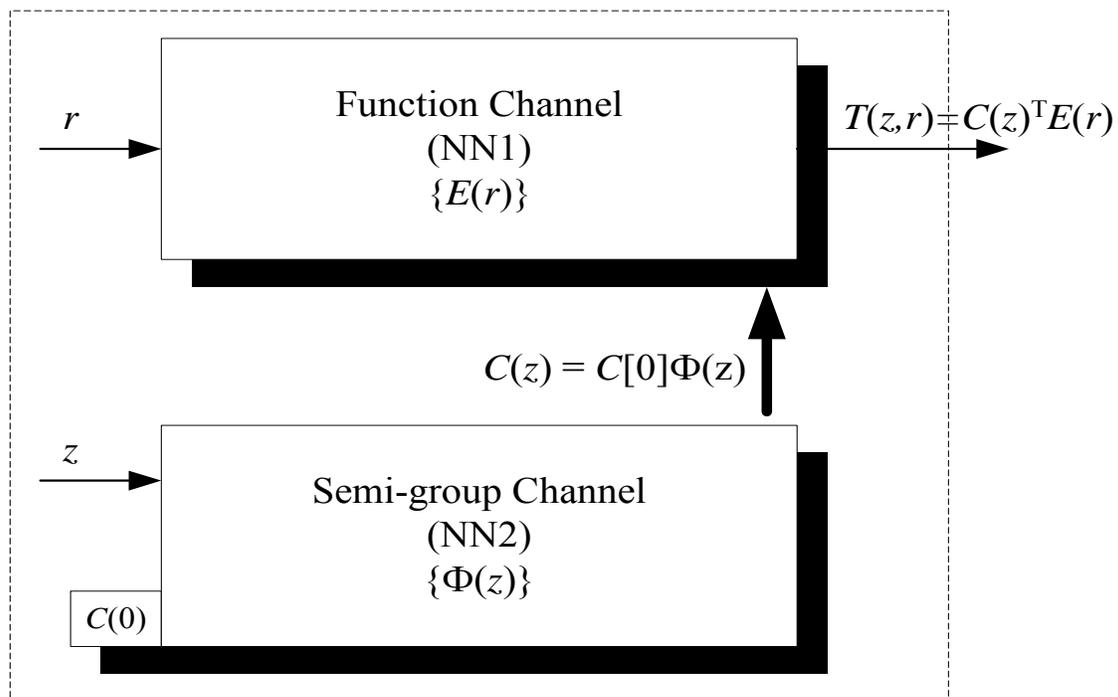

Fig. 2. System-type architecture.

22

The function channel can have a Radial Basis Function (RBF) architecture [8]. It consists of *n* RBF networks, each one of which implements one orthonormal vector of an *n*-dimensional basis set of vectors $E(r)$. The outputs of the orthonormal vectors are (internally) linearly summed so that the channel spans an *n*-dimensional function space. The coefficients which determine the linear sum and thereby define the specific function being implemented is supplied by the semigroup channel. Up to this point, the operation of the RBF channel parallels the idea used by Phan and Frueh [9]. One of the essential differences between their approach and the present proposed approach is that the former requires prior engineering knowledge for selecting the basis vectors, and the latter approach requires no such knowledge. One advantage that RBF networks have over other architectures is that their functionality can be given an explicit mathematical expression in which the neuron activation functions act as Green's functions [10], [11]. This makes these networks amenable to design rather than training. Another advantage is that they function as universal approximators [8]. The semigroup channel can be adapted from the Diagonal Neural Network (DRNN) [12], [13] or the Elman architecture [14], in which the input is split into a dynamic scalar component *z* and one static vector component, the vector $C(0)$. The output is a vector $C(z)$, which is related to the dynamic input *z* and to the static input $C(0)$ by the semigroup property: $C(z) = \Phi(z)C(0)$, where $\Phi(z_1 + z_2) = \Phi(z_1)\Phi(z_2)$. (Refer to Fig. 2).

3.2.6 Learning Algorithm of Proposed System-type NN

The first component of the system, namely the Function Channel, since it is composed of RBF components, can be designed, rather than trained. The second component, the Semigroup Channel, can be trained in the new way illustrated below. During training, the semigroup channel receives as input a preliminary coefficient vector $C(z)$ and produces a smoothened coefficient vector $\tilde{C}(z)$. That is, the primary objective of training is to replicate (and, if necessary, to smoothen) the vector $C(z)$ with a vector $\tilde{C}(z)$ which has the following semigroup property [15]: $\tilde{C}(z) = \Phi(z)\tilde{C}(0)$, where $\tilde{C}(z) \equiv [\tilde{c}_1(z), \tilde{c}_2(z), ..., \tilde{c}_n(z)]^T$ and $\Phi(z)$ is an *n*x*n* matrix that satisfies: $\Phi(z_1 + z_2) = \Phi(z_1)\Phi(z_2)$. However, there is a secondary objective of training; the channel must also "replicate" the semigroup property of the trajectory by gradually acquiring a semigroup property of its own, in weight space. The existence of this acquired semigroup property in weight space becomes the basis for extrapolation. In order to elicit this gradual acquisition of the semigroup property, it is necessary that the training in this second step (semigroup tracking) occur in a gradual manner, as shown in Fig. 3. In Fig. 3, the entire trajectory is split into successively-longer sub-trajectories.
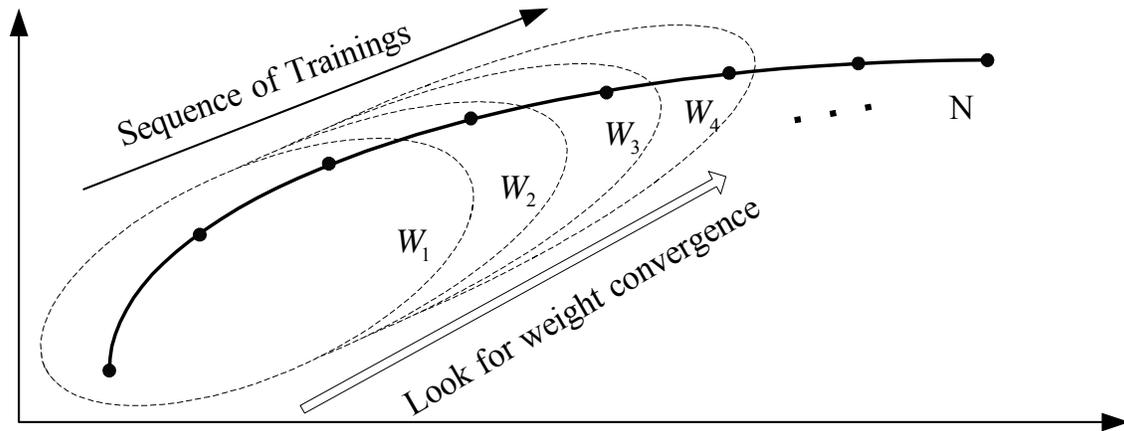
Fig. 3. Overview of new training algorithm.

3.2.7 System Modeling

The modeling and extrapolation problem is formulated as follows. Given a set of empirical data for which there is no analytic description, first develop an analytic model for the data, and then extrapolate the model along one specific axis. System modeling is achieved through a technique referred to as algebraic decomposition. Algebraic decomposition is an operation which is applied to a given function $T(r, z)$, for the purpose of representing it in a form that contains a semigroup: $T(r, z) = T_z(r) = C(z)^T E(r)$, where $E(r)$ provides the algebraic basis for the representation of each member of the parameterized function $\{T_z(r)\}$. The essential value of algebraic decomposition is that when it is applied to the class of functions that will be considered in this proposed research, it always produces a semigroup property for the coefficient vector.

3.2.8 Extrapolation

Extrapolation involves only the coefficient vector and the Elman neural network (the semigroup channel). At the uppermost level, the idea is to train the neural network to replicate the coefficient vector (produced by the previous system modeling effort) in such a way that it is additionally replicating the semigroup property, which is responsible for generating the coefficient vector by acquiring a semigroup property of its own in weight space. As a comparison, some other recent extrapolation attempts are given in [16]. One current method, which also attempts to build a universal framework for extrapolation, occurs in various forms in nonlinear control theory and is collectively called "continuation methods." These methods have been in existence for some time, but are only recently receiving attention [17].

3.3 Simulation and Estimation Results

The following illustrates simulation results of the application of the proposed method to the prediction (extrapolation) of temperature data from a boiler furnace of dimensions comparable to that found in a power plant. The data represents "raw data" furnished by the Penn State Energy

Institute. The geometry of the furnace is cylindrical with the z-axis along the furnace axis, and with r going from one wall to the other wall. (Note that r is a diameter, not a radius.) A simulation will be performed on the configuration below, where there are 25 probes, each one providing 11 readings. The extrapolation will be simulated in the region occupied by probes 25 to 30, Fig. 4. The results of the extrapolation will be compared to given raw data in that region. The temperature distribution is shown in Fig. 5.
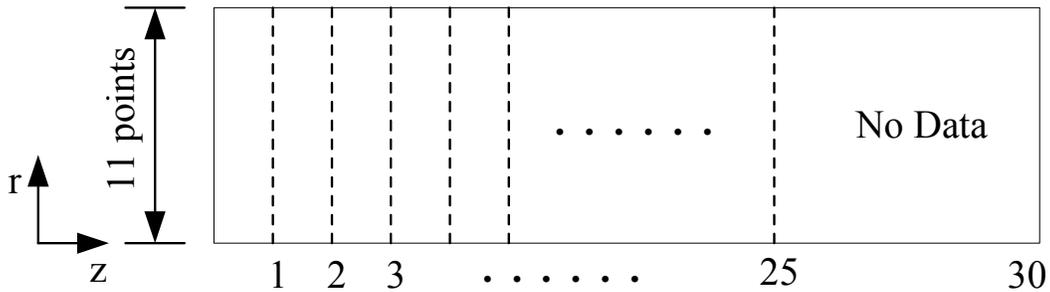

Fig. 4. Temperature probe configuration for the furnace.
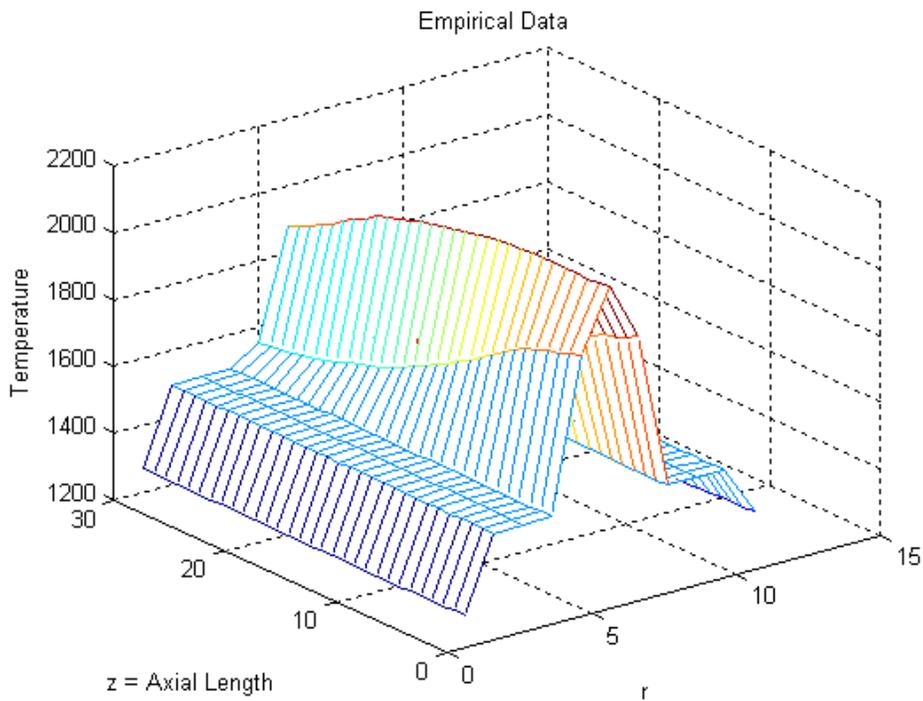
Fig. 5. Temperature distribution for the furnace.

The preliminary (rough) coefficient vector and the basis vectors produced by the RBF network are shown in Fig. 6. The use of this rough coefficient vector together with the basis set of vectors can produce the computed temperature distribution shown in Fig. 7. The Elman neural network then smoothens the preliminary coefficient vector, as shown in Fig. 8 (only the first two coefficients are shown).
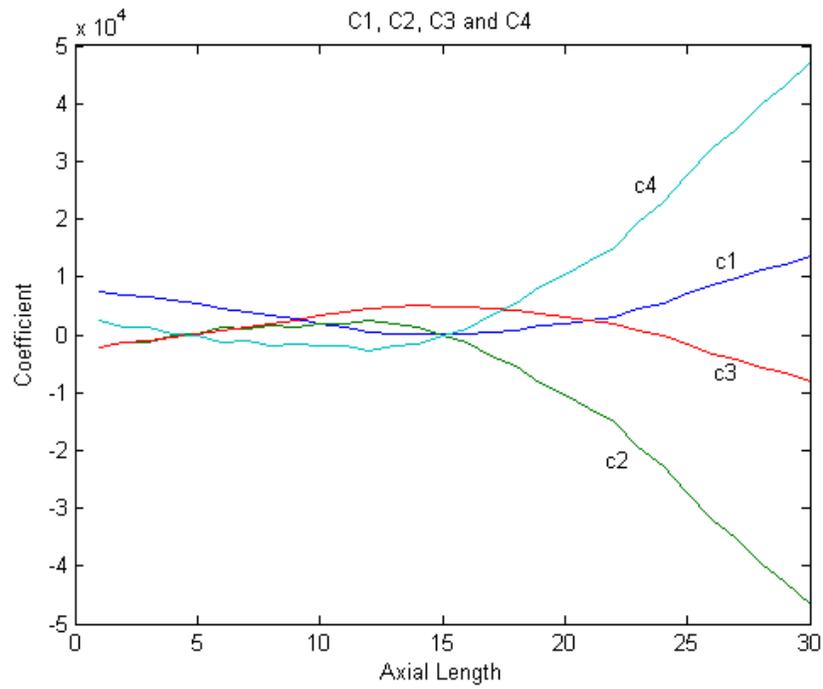
Fig. 6a. Preliminary coefficient vector set.
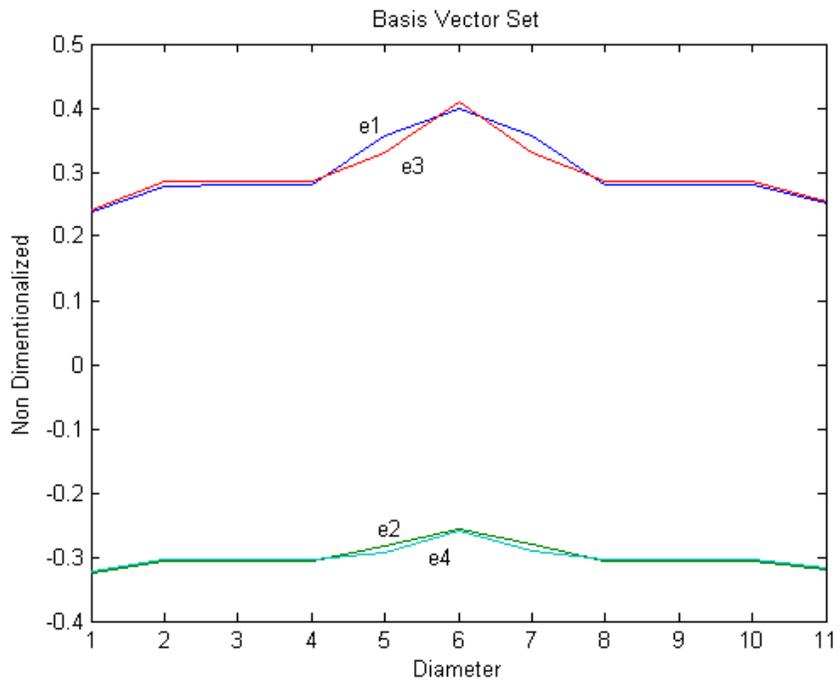

Fig. 6b. Basis vector set.
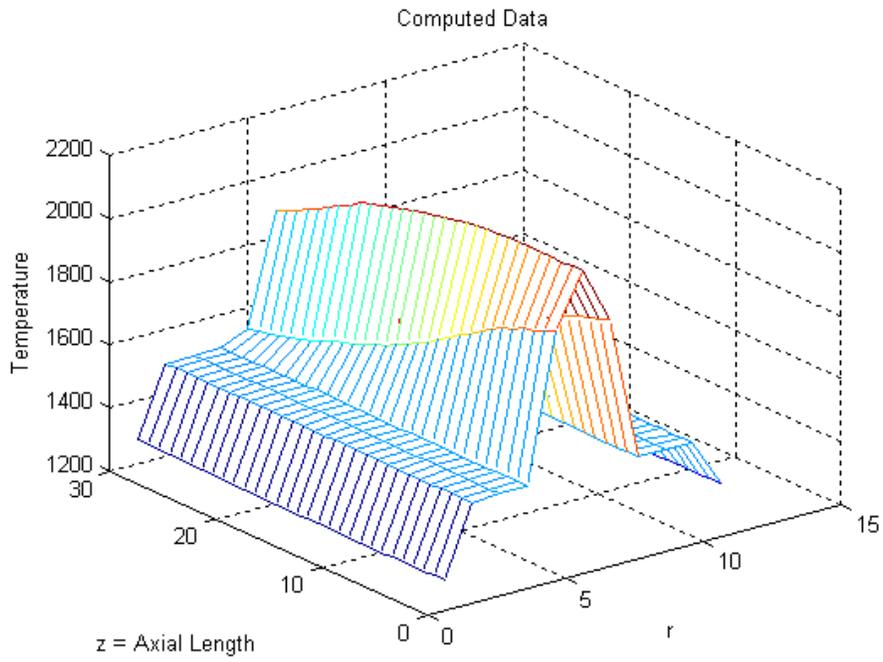
Fig. 7. Computed temperature.
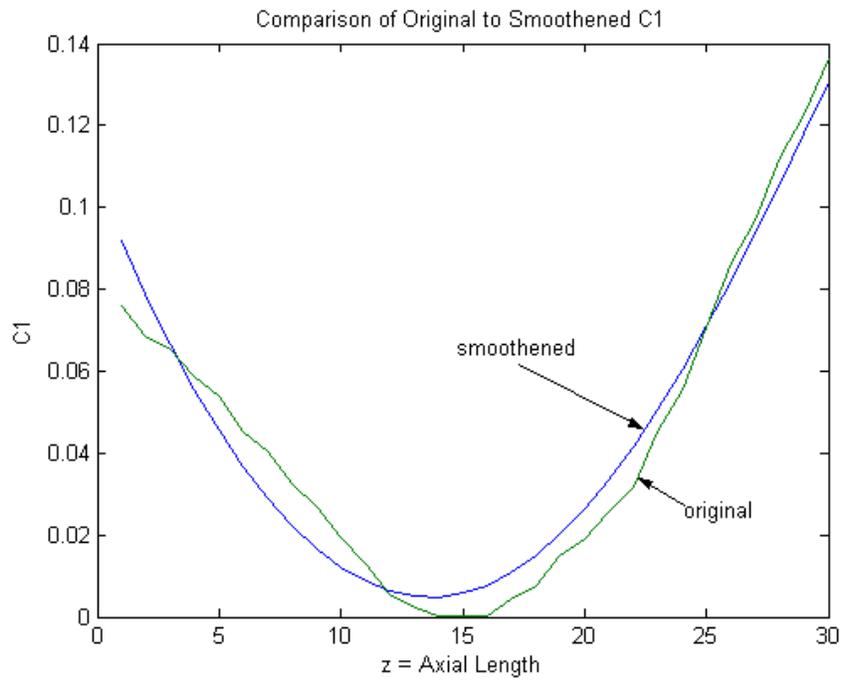
Fig. 8a. Comparison of original to smoothened coefficient vectors (only first two coefficients are shown).
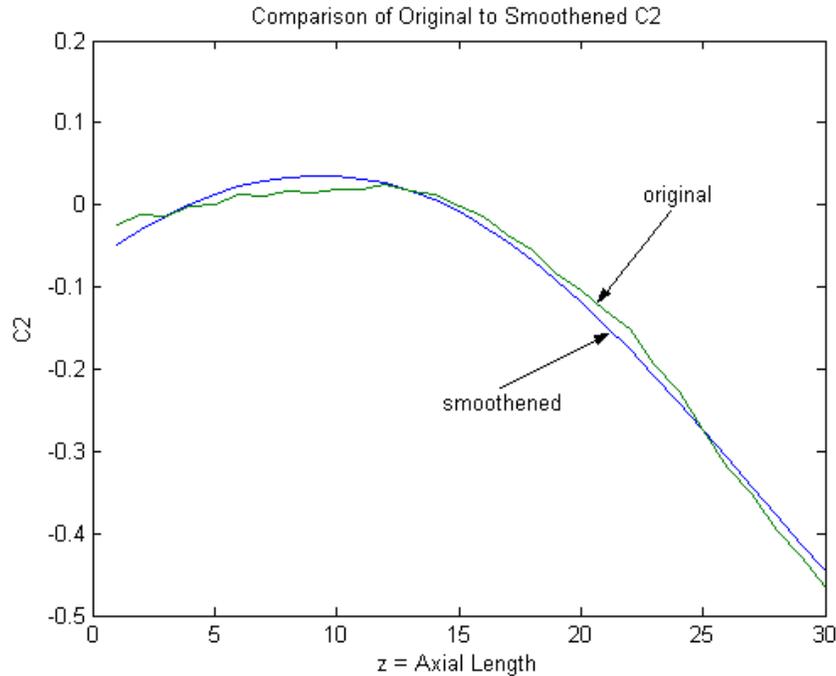
Fig. 8b. Comparison of original to smoothened coefficient vectors (only first two coefficients are shown).

The possibility for extrapolation begins by checking for weight convergence as training is performed along the coefficient vector. In this case, weight convergence occurs as this training is repeated over successively longer intervals (refer Fig. 3). It is this weight convergence, which becomes the basis for extrapolation. These are shown in Fig. 9.

In this case, because of the smoothness, the possibility for extrapolation exists and the next step is to apply an extrapolation test in which the trailing end of the weight change sequence (produced by training) is replaced by an equivalent weight change sequence based on a rule that generates a semigroup. Based upon an observation of the weight change sequence on the interval from 15 to 20, a semigroup-based rule for weight change is formulated and applied to the interval from 20 to 25, as a test. Extrapolation (to the region where no data were assumed) consists of the autonomous continuation of the rule for weight change, which was derived during the extrapolation test. These results are shown in Fig. 10 below (only the first two coefficients are shown).
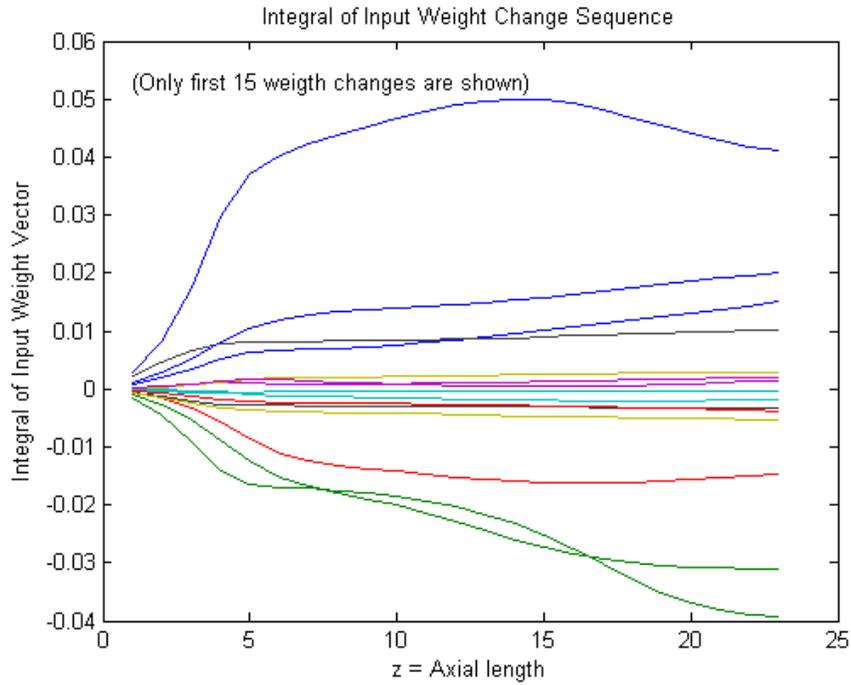
Fig. 9. Integral of input weight change sequence.
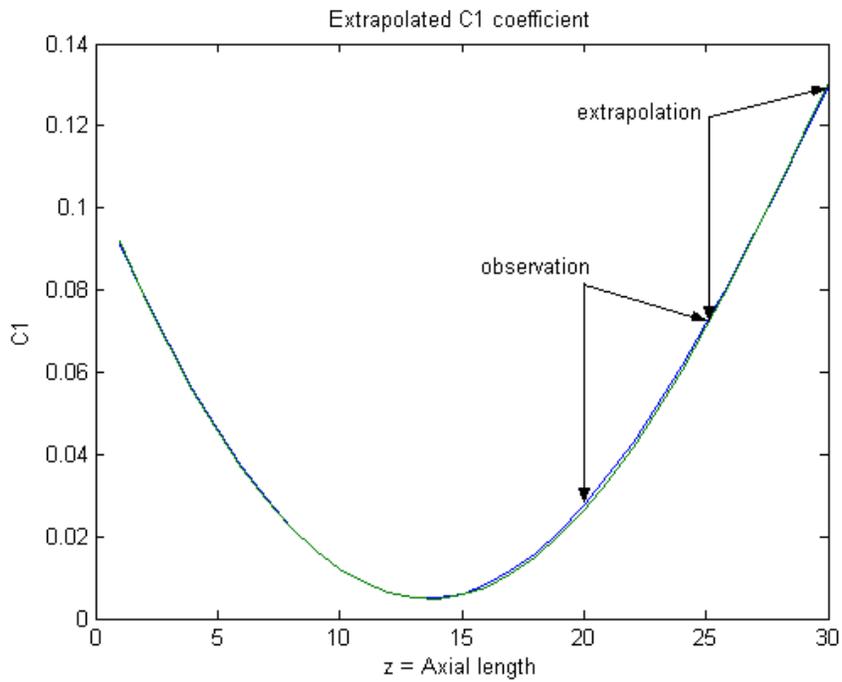
Fig. 10a. Extrapolation results for C1.
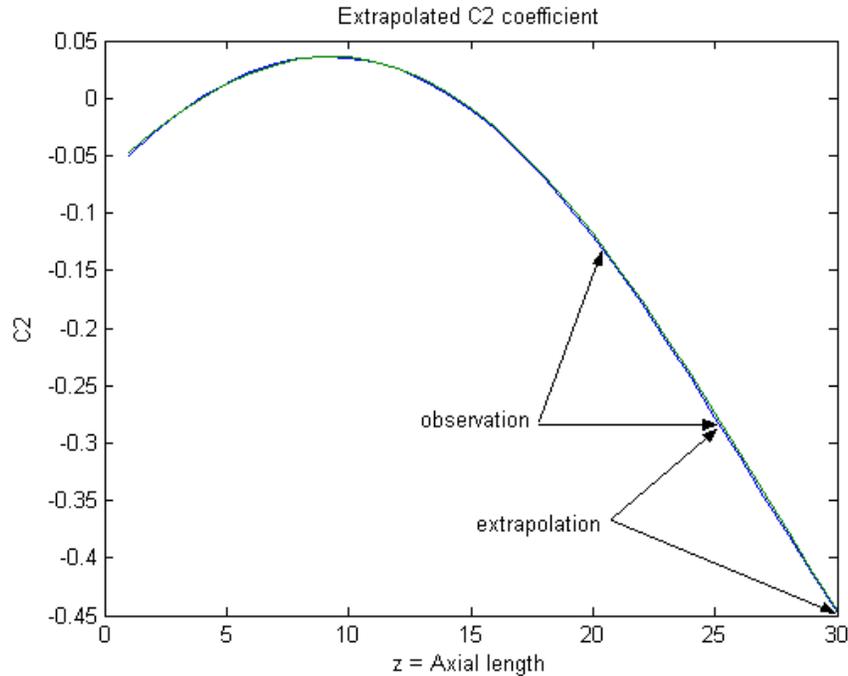
Fig. 10b. Extrapolation results for C2.

3.4. Conclusions

In this research, we investigate a mathematical approach to extrapolation of the temperature distribution within a power plant boiler facility, using a combination of a modified neural network architecture and semigroup theory. Given a set of empirical data with no analytic expression, we first develop an analytic description and then extend that model along a single axis. This can be achieved by using the algebraic decomposition to obtain an analytic description of empirical data in a specific form, called the semigroup form, which involves the product of a coefficient vector and a basis set of vectors. If this form can be achieved, the describing aspect is simplified because the description of the coefficient vector is decoupled from the description of the basis vector. Additionally, each component of the coefficient vector and each component of the basis set of vectors can be described individually.

3.5 Future Work Plan

The concept of the system-type neural networks will be applied to develop an intelligent monitoring system for estimating temperature distribution in boiler furnace.

3.6 References

[1]   K. Li and S. Thompson, "A cascaded neural network and its application to modeling power plant pollutant emission", *Proceedings of the 3rd World Congress on Intelligent Control and Automation*, pp. 992–997, Vol. 2, 28 June-2 July 2000.

[2]   K. Y. Lee, J. P. Velas, and B. H Kim, "Development of an Intelligent Monitoring System with High Temperature Distributed Fiberoptic Sensor for Fossil-Fuel Power Plants", *IEEE Power Engineering Society General Meeting*, pp. 1350-1355, Jun 6-10, 2004.

[3]   N. U. Ahmed, *Semigroup theory with applications to systems and control,* Longman Scientific & Technical, Harlow, 1991.

[4]   R. Jacobs and M. Jordan, "A Competitive Modular Connectionist Architecture", *Advances in Neural Information Processing Systems*, Vol. 3, pp. 767-773, Morgan-Kaufmann, Cal., 1991.

[5]   Atiya, R. Aiyad, and S. Shaheen, "A Practical Gated Expert System Neural Network", *IEEE International Joint Conference on Neural Networks*, Vol. 1, pp. 419-424, 1998.

[6]   H. Tanabe, *Equations of Evolution*, Pitman Publishing Ltd., London, 1979.

[7]   R. Padhi and S. N. Balakrishnan, "Proper orthogonal decomposition based feedback optimal control synthesis of distributed parameter systems using neural networks", *Proceedings of the 2002 American Control Conference*, 2002, pp. 4389–4394, Vol. 6, pp. 8-10, May 2002.

[8]   S. Haykin, *Neural Networks,* 2nd ed., Prentice Hall, N.J., 1999.

[9]   M. Q. Phan and J. A. Frueh, "Learning Control for Trajectory Tracking using Basis Functions", *Proceedings of the 35th IEEE Conference on Decision and Control*, pp. 2490-2492, Dec. 1996.

[10]   A.N. Tikhonov, "On regularization of ill-posed problems", *Doklady Akademii Nauk USSR,* vol. 153, 1973.

[11]   A.N. Tikhonov, "On solving incorrectly posed problems and method of regularization," *Doklady Akademii Nauk* vol. 151, USSR, 1973.

[12]   C. C. Ku, K.Y. Lee, and R.M. Edwards, "Improved Nuclear Reactor Temperature Control Using Diagonal Recurrent Neural Networks," *IEEE Trans. on Nuclear Science*, Vol. 39, pp. 2298-2308, December 1992.

[13]   C. C. Ku and K.Y. Lee, "Diagonal Recurrent Neural Networks for Dynamic Systems Control*," IEEE Trans. on Neural Networks,* Vol. 6, pp. 144-156, January 1995.

[14]   J. Elman., "Finding Structure in Time", *Journal of Cognitive Science*, Vol. 14, pp. 179-211, 1990.

[15]   Miyadera, *Nonlinear Semigroups*, American Mathematical Society, Providence, R.I., 1992.

[16]   Z. Altman and R. Mittra, "A technique for extrapolating numerically rigorous solutions of electromagnetic scattering problems to higher frequencies and their scaling properties", *IEEE Transactions on Antennas and Propagation*, Vol.: 47, No. 4, April 1999.

[17]   S. Richter and R. de Carlo, "Continuation methods: Theory and applications", *IEEE Transactions on Automatic Control*, Vol. 28, pp. 660-665, 1983.

RELATED TECHNICAL PUBLICATIONS

<u>Refereed Journal Papers</u>

1. Y. Yang, K. Chung, S. Yin, Z. Liu, and Q. Wang, "Analysis of volume holographic long period grating in photonic nanostructured fibers and waveguides," Optical Engineering, Vol. 43, pp.2003-2008 (2004).

2. D. Komisarek, K. Reichard, D. Merdes, D. Lysak, P.Lam, S. Wu, and S. Yin, "High-performance nonscanning Fourier-transform spectrometer that uses a Wollaston prism array," Applied Optics, Vol. 43, pp.3983-3988, 2004.

3. D. Komisarek, K. Reichard, and S. Yin, "Enhancing the performance of non-scanning Fourier transform spectrometer by compensating manufacturing defects inherent to a Wollaston prism array," Optics Communications, Volume 238, pp. 85-90 (2004).

4. Bo Wang, Ruyan Guo, Shizhuo Yin and Francis Yu, "Chemical sensing with Hetero-Core Fiber Specklegram," Journal of Holography and Speckle 1, 53 (2004).

5. K. Shi, P. Li, S. Yin, and Z. Liu, "Chromatic confocal microscopy using supercontinuum light," Optical Express, Vol. 12, No. 10, pp. 2096-2101 (2004).

6. Kun-Wook Chung and Shizhuo Yin, "Analysis of a widely tunable long-period grating by use of an ultra thin cladding layer and higher-order cladding mode coupling," Optics Letters, Vol. 29, pp.812-814 (2004).

7. Kun-wook Chung and Shizhuo Yin, "A highly nonlinear dispersion shifted fiber with 9.3 mm2 effective area and low loss for all fiber wavelength converter," Microwave and Optical Technology Letters," pp. 153-156 (2004).

Refereed Conference Proceedings

1. K. Y. Lee, J. P. Velas, and B. H Kim, "Development of an Intelligent Monitoring System with High Temperature Distributed Fiberoptic Sensor for Fossil-Fuel Power Plants", *IEEE Power Engineering Society General Meeting*, pp. 1350-1355, Jun 6-10, 2004.

2. Stuart (Shizhuo) Yin, Sung-Hyun Nam, Yi Yang, Chun Zhan, and Kun-Wook Chung, "Innovative Fiber Optic Gratings: Fabrications and Applications," Proceedings of International Symposium on Advances and Trends in Fiber Optics and Applications, October 11-15, 2004, Chongqing University, Chongqing, China. (**Invited Paper**)

3. S. Yin, C. Hahn*, J. Lee*, B. Wang*, and Q. Wang, „Design and implementation of an all-fiber ultra-fast widely tunable wavelength filter (invited)," Proceedings of SPIE on Information Optics and Photonics Technology, SPIE, 5643, pp. *-* (2004) (Principal author; second, third, and fourth authors supervised by candidate) (**Invited paper**)

4. S. Nam, C. Zhun, S. Yin, "High temperature distributed fiber optic sensors," Proceeding s of SPIE on Fiber Optic Sensors, SPIE, 5634, pp. *-* (2004) (First and second authors supervised by candidate) (**Invited paper**)

5. W. Su, Y. Hsu, C. Kuo, H. Chan, and S. Yin, "Design and fabrication of digital dual-freuqnecy patterns for projected fringe profilometry, SPIE 5606-20, Philadelphia, PA, Oct. 27, 2004.

6. S. Yin, B. Wang, C. Luo, Q. Wang, K. Reichard, and D. Lysak, "Development of harsh environment electro-optic polymer and their applications to tunable photonic devices," IEEE LEOS Summer Topic meeting on Optical Interconnects & VLSI Photonics, MB4.2, San Diego, CA, June 28, 2004.

7. S. Nam, Chun Zhan, and S. Yin, "Recent advances on fabricating in-fiber gratings in single crystal sapphire fiber," SPIE 5560, pp.147-155, Denver, CO, Aug., 2004.

8. Jon Lee, B. Wang, C. Hahn, K. Reichard, D. Ditto, D. Glista, Q. Wang, and S. Yin, "Harsh environment electro-optic polymer and its application to in-fiber tunable filter," SPIE 5560, pp. 52-63, Denver, CO, Aug., 2004.

9. B. Wang, Y. Yang, Y. Liu, S. Yin, R. Guo, P. Ruffin, "Fiber optic sensors using photonic crystal fiber embedded heterofiber structures," SPIE 5560, pp.284-294, Denver, CO, Aug., 2004.

10. Wei-Hung Su, Cho-Yo Kuo, and Shizhuo Yin, "Design and fabrication of various digital fringe patterns for projected fringe profilometry," SPIE 5560, pp. 193-203, Denver, CO, Aug., 2004.

11. K. Reichard, S. Yin, C. Hahn, J. Lee, B. Wang and Q. Wang, "An athermal design for an all-fiber, ultra fast, widely tunable wavelength filter," Avionics, Fiber-Optics and Photonics Workshop, Workshop Notes, ThP15, St. Louis Marriott Downtown, St. Louis, MO, 21-23 April 2004.

12. S. Yin, S. Nam, P. Ruffin, K. Reichard, "An investigation of a photonic bandgap based gyroscope and its application to Avionics, Avionics, Fiber-Optics and Photonics Workshop, Workshop Notes, ThP17, St. Louis Marriott Downtown, St. Louis, MO, 21-23 April 2004.

13. Sung-Hyun Nam, Jesus Chavez, and Shizhuo Yin, "Fabricating in fiber gratings in single crystal sapphire fibers," SPIE 5350, pp.58-65, San Jose, CA, Jan., 2004.

14. Shizhuo Yin, Thomas W. Gardner*, Fei Wu and Milind Cholker, "Optical combing to align photoreceptors in detached retinas," SPIE 5314, pp.298-305, San Jose, CA, Jan. 2004.

15. Yi Yang, KunWook Chung, Shizhuo Yin, Karl Reichard*, Zhiwen Liu, and Qing Wang[+], "Highly sensitive sensors using in-fiber gratings fabricated in photonic crystal nanostructures," SPIE 5360, pp.237-246, San Jose, CA, Jan., 2004.

REVIEW MEETING

We attended the annual review meeting held on June 2-3, 2004 in Pittsburgh, PA.